Enzymatic Mechanism of Low-Activity Mouse Alcohol Dehydrogenase 2[†]

Patrik Strömberg,[‡,§] Stefan Svensson,[‡,||] Kristine B. Berst,[⊥] Bryce V. Plapp,[⊥] and Jan-Olov Höög*[,‡]

Department of Medical Biochemistry and Biophysics, Karolinska Institutet, Stockholm, Sweden, and Department of Biochemistry, The University of Iowa, Iowa City, Iowa 52242

Received August 13, 2003; Revised Manuscript Received October 28, 2003

ABSTRACT: ADH2 is a member of one of the six classes of mammalian alcohol dehydrogenases, which catalyze the reversible oxidation of alcohols using NAD^+ as a cofactor. Within the ADH2 class, the rodent enzymes form a subgroup that exhibits low catalytic activity with all substrates that were examined, as compared to other groups, such as human ADH2. The low activity can be ascribed to the rigid nature of the proline residue at position 47 as the activity can be increased by ∼100-fold by substituting Pro47 with either His (as found in human ADH2), Ala, or Gln. Mouse ADH2 follows an ordered bi-bi mechanism, and hydride transfer is rate-limiting for oxidation of benzyl alcohols catalyzed by the mutated and wild-type enzymes. Structural studies suggest that the mouse enzyme with His47 has a more closed active site, as compared to the enzyme with Pro47, and hydride transfer can be more efficient. Oxidation of benzyl alcohol catalyzed by all forms of the enzyme is strongly pH dependent, with p*K* values in the range of 8.1−9.3 for turnover numbers and catalytic efficiency. These p*K* values probably correspond to the ionization of the zinc-bound water or alcohol. The p*K* values are not lowered by the Pro47 to His substitution, suggesting that His47 does not act as a catalytic base in the deprotonation of the zinc ligand.

The mammalian alcohol dehydrogenases (EC 1.1.1.1) constitute a family of dimeric zinc metalloenzymes that catalyze the reversible oxidation of alcohols using NAD^+ as a cofactor (*1*, *2*). At present, six classes of ADH[1] (ADH1−ADH6) with structurally distinct forms have been discovered in mammals (*3*). The enzymatic properties of ADHs have been extensively studied, and the horse liver ADH displays a predominantly ordered kinetic mechanism with coenzyme binding preceding binding of the substrate (*4*, *5*). The hydride transfer from the zinc-bound alcohol to the nicotinamide ring of the coenzyme apparently follows deprotonation of the alcohol substrate (*6*).

ADH2 was isolated as the π-subunit of human liver alcohol dehydrogenase and described as one of the ADH isoforms contributing to ethanol metabolism (*7*, *8*). More recent studies have established human ADH2 as an enzyme mainly expressed in liver and with a preference for unsaturated hydrophobic alcohols and aldehydes such as noradrenaline metabolites, 4-hydroxyalkenals, and ω-hydroxy fatty acids (*9*−*13*). Surprisingly, mouse and rat livers show no characteristic ADH2 activity. However, the enzymes are readily expressed from the cDNAs for rodent ADH2 orthologs, but they show poor catalytic efficiency for all the substrates that were examined (*14*, *15*). The activity of these enzymes can be improved significantly by replacing the unusual Pro47 with His (*15*). Arg47 typically interacts with the pyrophosphate of the coenzyme in other ADHs. His is present in some ADHs, and Gly is found in ADH1A. Substitutions at that position result in considerable changes in catalytic properties (*16*−*20*). Three-dimensional structures of mouse ADH2 suggest that His47 might function as a catalytic base in a proton relay connecting the substrate with the bulk solvent (*21*). Moreover, the structures indicate that changing Pro47 to His may cause coenzyme binding that is more favorable for efficient catalysis (*21*).

Because the kinetic mechanism of each alcohol dehydrogenase should be established, we used both transient and steady-state kinetic analyses to elucidate the mechanism of ADH2. In addition, rate-limiting steps were explored by use of isotope effects, and pH dependency studies were used to evaluate the contribution of residue 47 to acid−base catalysis.

EXPERIMENTAL PROCEDURES

Expression Plasmid Constructs and Site-Directed Mutagenesis. The full-length coding region for mouse ADH2 was isolated and subcloned into the pET29 expression vector (Novagen) as described previously (*15*). A double-stranded plasmid was prepared with the Flexiprep kit (Amersham Biosciences) for mutagenesis of mouse ADH2 cDNA. Reagents in the transformer site-directed mutagenesis kit (Clontech) and mutagenesis primers (5′-GCCACGTGTGTGTGCGCTACTGACATCAATG-3′ and 5′-GCCACGTGTGTGTGCCAGACTGACATCAATGCC-3′) were used to alter the codon for Pro at position 47 to those for Ala and

[†] This work was supported by grants from the Swedish Alcohol Research Fund, the Karolinska Institutet, and the United States Public Health Service, National Institutes of Health Grant AA00279.

* To whom correspondence should be addressed: Department of Medical Biochemistry and Biophysics, Karolinska Institutet, SE-171 77 Stockholm, Sweden. Telephone: +46-8-524 87740. Fax: +46-8-338 453. E-mail: jan-olov.hoog@mbb.ki.se.

[‡] Karolinska Institutet.

[§] Present address: AstraZeneca Biotech Laboratory, SE-151 83 Södertälje, Sweden.

[||] Present address: Department of Structural Chemistry, Biovitrum AB, SE-112 76 Stockholm, Sweden.

[⊥] The University of Iowa.

[1] Abbreviation: ADH, alcohol dehydrogenase.

10.1021/bi0354482 CCC: $27.50
Published on Web 01/13/2004

Gln (nucleotides corresponding to the changed codons are underlined). Selection of the mutants was based on the elimination of the unique *Sal*I site of the pET29 vector (*22*). The Pro47His mutant enzyme was generated as described previously (*15*). The sequences were analyzed with the BigDye terminator cycle sequencing kit (PE/Applied Biosystems) using fluorescent dNTPs and plasmid or sequence specific primers to confirm the presence of the correct mutations and the absence of any unexpected mutations in the cDNA.

Preparation of Enzymes. The ADH2 enzymes were expressed heterologously and isolated as described previously (*15*). Briefly, the recombinant enzymes were purified by anion-exchange and affinity chromatography before being desalted and exchanged into 10 mM sodium 4-(2-hydroxyethyl)-1-piperazineethanesulfonate buffer (pH 7.5) by gel filtration. The enzymes were homogeneous as determined by polyacrylamide gel electrophoresis in the presence of sodium dodecyl sulfate. Protein concentrations were determined with the Bio-Rad protein assay, standardized with bovine serum albumin complemented with amino acid analysis on an Amersham Pharmacia Biotech Alpha Plus analyzer.

Steady-State Kinetics. The activity of wild-type and mutant mouse ADH2 enzymes was determined in a standard assay with 5 mM benzyl alcohol and 2.4 mM NAD^+ in 0.1 M sodium glycine buffer (pH 10) at 25 °C, by measuring the change in absorbance at 340 nm for NADH production ($\epsilon = 6220\ M^{-1}\ cm^{-1}$). $LiNAD^+$ (grade I) and Na_2NADH (grade I) were obtained from Roche Applied Science. Benzyl alcohol and benzaldehyde were redistilled before use. Initial velocity and inhibition studies monitored the absorbance of NADH or the fluorescence obtained by excitation at 340 nm and emission at 460 nm. Substrate concentrations were varied over a 7−9-fold range encompassing the K_m value for the particular enzyme, and inhibitor concentrations were varied over a 3−4-fold range. The data were fitted to the appropriate equations using the programs of Cleland (*23*) or Sigma Plot/Enzyme Kinetics (SPSS).

pH Dependence Studies. The pH dependencies for the steady-state reactions of benzyl alcohol were measured with 2.4 mM NAD^+ and varied concentrations of substrate. Buffers consisted of 10 mM $Na_4P_2O_7$, 0.25 mM EDTA, and sufficient H_3PO_4, NaH_2PO_4, and Na_2HPO_4 to produce the desired pH and a final ionic strength of 0.1 in the range of pH 6.0−9.0 (*17*). Buffers at pH 9.5 and 10.0 consisted of 10 mM $Na_4P_2O_7$, 0.25 mM EDTA, and 5 mM sodium carbonate for buffering capacity. The buffers were made double-strength and diluted 2-fold in the reaction mixture to minimize the incubation of NAD^+ at high pH. Enzymes were stored in 10 mM sodium HEPES (pH 7.5). The data for pH dependence were fitted to the following equations:

$$k_{obs} = k_1/(1 + [H^+]/K_a) \quad (1)$$

$$k_{obs} = (k_2 + k_1K_a/[H^+])/(1 + K_b/[H^+] + [H^+]/K_a) \quad (2)$$

These equations are based on the general model below where E represents enzyme, K_a and K_b are acid dissociation constants, and k values are rate constants. The equations only describe the form of dependence and do not imply that the same groups are ionizing in each reaction:

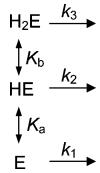

Transient Kinetics. For transient kinetic experiments, we used a BioLogic SFM3 stopped-flow instrument with a dead time of 2.5 ms. The data were analyzed with the BioKine Software. Reactions were studied at 25 °C in 100 mM potassium phosphate buffer (pH 7.5) unless stated otherwise. NADH association was followed by the quenching of intrinsic protein fluorescence. The oxidation of octanol and reduction of benzaldehyde were followed by the change in absorbance at 328 nm, the isosbestic point for free and bound NADH. The kinetic simulation program KINSIM and the automatic fitting routine FITSIM (*24*) were used to estimate microscopic rate constants by fitting several transient progress curves simultaneously.

RESULTS

Steady-State Kinetic Studies. The kinetic constants for wild-type and mutated mouse ADH2 were elucidated with steady-state kinetics experiments. Initial velocity experiments were performed for oxidation of benzyl alcohol and reduction of benzaldehyde by varying the substrate concentration at different fixed coenzyme concentrations. These substrates were chosen because they are among the best substrates for this enzyme (*15*). Intersecting double-reciprocal plots were obtained (Figure 1). All data fitted best to a sequential bi reaction (*23*), and the kinetic constants are presented in Table 1. All three substitutions in mouse ADH2 increased the rate of turnover for alcohol oxidation by ~2 orders of magnitude, to values similar to those for the native human enzyme (*15*). Notably, this shows that the activation of mouse ADH2 is not dependent on a catalytic base in either position 47 or 51 (mouse ADH2 has Asn51). However, the substitution of Pro47 with any other residue increases the dissociation constant for the coenzyme substantially. For reduction of benzaldehyde, the Pro47His substitution increased the turnover number by 5-fold and the dissociation constant for NADH by 10-fold (Table 1). For the two other mutated enzymes, substrate inhibition occurred at benzaldehyde concentrations of $<100\ \mu M$, and kinetic constants were not determined.

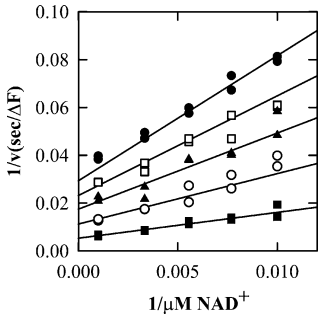

FIGURE 1: Initial velocity studies for the oxidation of benzyl alcohol by the mouse Pro47Gln mutant at pH 7.5 and 25 °C. The double-reciprocal plot displays an intersecting pattern with varied NAD^+ concentrations with 0.20 (●), 0.26 (□), 0.36 (▲), 0.62 (○), and 2.0 mM benzyl alcohol (■). Data were fitted to a sequential bi mechanism (*23*), and the results are listed in Table 1.

Table 1: Steady-State Kinetic Constants for Wild-Type and Mutated Mouse ADH2 Enzymes[a]

kinetic parameter[b]	wild type	Pro47Ala	Pro47Gln	Pro47His
K_a (μM)	2.8 ± 0.4	120 ± 30	240 ± 50	100 ± 20
K_b (mM)	3.2 ± 0.4	1.3 ± 0.3	2.0 ± 0.3	3.9 ± 0.3
K_p (mM)	0.84 ± 0.07	ND[e]	ND[e]	0.47 ± 0.09
K_q (μM)	1.0 ± 0.1	ND[e]	ND[e]	6.7 ± 0.1
K_{ia} (μM)	4.1 ± 0.8	34 ± 12	170 ± 30	210 ± 20
K_{iq} (μM)	1.6 ± 0.2	ND[e]	ND[e]	15 ± 3
V_1/E_t (s^{-1})	0.016 ± 0.003	1.4 ± 0.2	1.1 ± 0.1	1.2 ± 0.1
V_2/E_t (s^{-1})	1.9 ± 0.1	ND[e]	ND[e]	9.0 ± 0.9
K_{eq} (pM)[c]	27	ND[e]	ND[e]	37
specific activity (s^{-1})[d]	0.42	3.9	5.4	7.1

[a] Kinetic constants were determined at 25 °C in 0.1 M potassium phosphate and 0.25 mM EDTA buffer (pH 7.5). Measurements were conducted fluorometrically under initial velocity conditions. For the forward reaction, benzyl alcohol and NAD^+ concentrations were both varied, and for the reverse reaction, benzaldehyde and NADH concentrations were varied. Data were fitted to a sequential bi reaction (*23*), and values are presented ± standard errors. [b] The kinetic constants K_a, K_b, K_p, and K_q represent the Michaelis constants for NAD^+, benzyl alcohol, benzaldehyde, and NADH, respectively. K_{ia} and K_{iq} are the dissociation constants for NAD^+ and NADH, respectively. V_1/E_t is the k_{cat} for the forward reaction and V_2/E_t for the reverse. [c] K_{eq} is calculated from the Haldane equation, $V_1K_pK_{iq}[H^+]/V_2K_bK_{ia}$. [d] Specific activity based on standard assays described in Experimental Procedures. [e] Not determined due to substrate inhibition.

Table 2: Dead-End Inhibition Patterns for Wild-Type Mouse ADH2[a]

inhibitor	substrate: varied	substrate: fixed	pattern	K_i (μM)[b]
cyclohexylformamide (0.03−0.10 mM)	benzaldehyde (0.24−2.2 mM)	NADH (0.1 mM)	C	35 ± 3
cyclohexylformamide (10−50 mM)	NADH (1−5 μM)	benzaldehyde (0.88 mM)	UC	72 ± 9
octanoic acid (25−100 μM)	octanol (62−500 μM)	NAD^+ (1 mM)	C	37 ± 2
octanoic acid (25−100 μM)	NAD^+ (2−14 μM)	octanol (0.48 mM)	UC	26 ± 3

[a] Inhibition constants were determined at 25 °C in 0.1 M potassium phosphate buffer (pH 7.5) by fluorometry or spectroscopy under initial velocity conditions. Data were fitted to the equations for competitive (C) or uncompetitive (UC) inhibition (*23*), and the best fit was chosen on the basis of a comparison of the statistical analysis. [b] The K_i values are corrected using the equation $K_i = K_{ii}/(1 + B/K_b)$ for the uncompetitive inhibition with a fixed concentration of substrate (*B* is the concentration of benzaldehyde or octanol) and the equation $K_i = K_{is}/(1 + K_{ia}/A)$ for competitive inhibition with a fixed concentration of coenzyme (*A* is the concentration of NAD^+ or NADH).

Dead-end inhibition experiments were performed to further elucidate the reaction mechanism and to determine whether the mechanism is ordered or random (Table 2). *N*-Cyclohexylformamide (an aldehyde analogue) is a competitive inhibitor against varied concentrations of benzaldehyde, but an uncompetitive inhibitor against varied concentrations of NADH (Figure 2). Likewise, octanoic acid is competitive against octanol as a substrate and uncompetitive against NAD^+. The K_i values were corrected for the effect of the concentration of the fixed substrate and agree within experimental error. These results are consistent with an ordered mechanism with coenzyme binding before substrate and not consistent with a simple rapid equilibrium random mechanism.

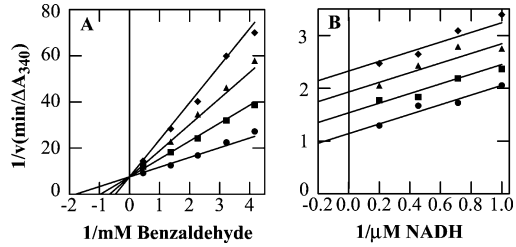

FIGURE 2: Dead-end inhibition of mouse ADH2 by *N*-cyclohexylformamide. The inhibition studies were performed at 25 °C in 0.1 M potassium phosphate and 0.25 mM EDTA buffer (pH 7.5). (A) The NADH concentration was 0.1 mM. Cyclohexylformamide concentrations were 0 (●), 30 (■), 60 (▲), and 100 μM (◆). (B) The benzaldehyde concentration was 0.86 mM. Cyclohexylformamide concentrations were 0 (●), 50 (■), 100 (▲), and 150 μM (◆). The data points are the average of duplicate assays.

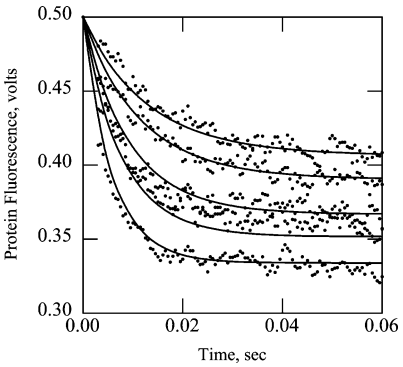

FIGURE 3: Binding of NADH to mouse ADH2. The enzyme (final concentration of 1 μN) was mixed with varied concentrations of NADH (2.5, 3.3, 5, 6.7, and 10 μM from top to bottom) in 0.1 M sodium phosphate and 0.25 mM EDTA buffer (pH 7.5) at 25 °C, and the decrease in protein fluorescence (λ_{ex} = 294 nm, λ_{em} = 310−384 nm) was measured with a BioLogic SFM3 stopped-flow instrument. The data were fitted with KINSIM/FITSIM (*24*) to the reversible reaction E + NADH ⇆ E−NADH with a relative fluorescence of 1.0 for the free enzyme and 0.56 ± 0.004, as a fitted parameter, for the E−NADH complex. The rate constant for the bimolecular association (k_{on}) was fitted at (1.39 ± 0.02) × 10^6 M^{-1} s^{-1}, and the rate constant for the dissociation (k_{off}) was 36.8 ± 0.7 s^{-1}.

Transient Kinetics Experiments. For wild-type mouse ADH2, transient oxidation of benzyl alcohol gave no burst phase prior to the steady-state reaction that is also observed in initial velocity experiments. These results are consistent with hydride transfer being rate-limiting for turnover. The binding of NADH was first-order, and the apparent rate constants were directly proportional to coenzyme concentration, yielding a rate constant of 14 μM^{-1} s^{-1} for the bimolecular reaction. Simulations of five transient reactions with different concentrations of NADH using FITSIM (Figure 3) yielded a k_{off} of 37 s^{-1}, which is significantly higher than the observed turnover number from steady-state kinetic measurements and therefore consistent with NADH dissociation not being a rate-limiting step for turnover of alcohol with this enzyme. NAD^+ association gave no significant quenching of protein fluorescence, and the reaction could therefore not be monitored.

Deuterium Isotope Effects. Isotope effects using deuterated benzyl alcohol were determined at pH 7.5 by steady-state kinetics measurements (Table 3). Large deuterium isotope effects on k_{cat} and k_{cat}/K_m were detected for all mouse ADH2 forms. The magnitudes of the values are consistent with

Table 3: Deuterium Isotope Effects on Benzyl Alcohol Oxidation for Mouse ADH2 Enzymes[a]

enzyme	$^{D}k_{cat}$	$^{D}k_{cat}/K_m$	enzyme	$^{D}k_{cat}$	$^{D}k_{cat}/K_m$
wild type	3.6	4.3	Pro47Gln	3.2	4.2
Pro47Ala	4.6	3.3	Pro47His	4.3	3.9

[a] Kinetic constants were determined from initial velocity experiments at 25 °C in 0.1 M potassium phosphate buffer (pH 7.5) with varied substrate concentrations and the NAD^+ concentration fixed at 2.4 mM. Propagated errors are ~14% of the values.

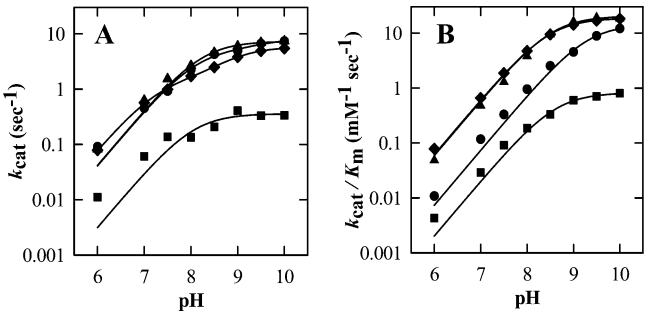

FIGURE 4: pH dependence of native and mutated mouse ADH2 enzymes. Kinetic constants were determined from initial velocity experiments at 25 °C with varied concentrations of benzyl alcohol and the NAD^+ concentration fixed at 2.4 mM. Panel A depicts the pH dependence for k_{cat} and panel B that for k_{cat}/K_m. The enzymes were the mouse wild type (■) and the Pro47His (●), Pro47Ala (◆), and Pro47Gln (▲) variants. The data were fitted to the logarithmic forms of the equations described in Experimental Procedures, and the p*K* values and limiting constants are listed in Table 4.

primary deuterium isotope effects resulting from breaking of the C−H bond in the transition state. This indicates that hydride transfer is rate-limiting for wild-type mouse ADH2 as well as for the more active mutated enzymes. Hence, the activation achieved by replacing Pro47 does not make the chemical catalysis step faster than coenzyme dissociation. Isotope effects were previously detected for the rodent ADH2 enzymes at pH 10 (*15*), and the data obtained in this study indicate that hydride transfer is rate-limiting for ADH2 catalysis at physiological pH.

pH Dependence Studies. The pH dependence for the steady-state oxidation of benzyl alcohol was determined in the pH range of 6.0−10.0. All ADH2 enzymes display a strong pH dependence on both turnover numbers and catalytic efficiencies, with the pH maxima well above physiological pH (Figure 4 and Table 4). For k_{cat}/K_m, the data for native ADH2 and mutated enzymes could be fitted to the equation for a single p*K* value where only the deprotonated form is active (eq 1). The data for the pH dependence of k_{cat} were also described well by eq 1, except that the data for the Pro47Ala enzyme were fitted somewhat better to eq 2. All ADH2 forms display p*K* values for k_{cat} and k_{cat}/K_m in the range of 8.1−9.3.

DISCUSSION

The mammalian ADH2 class of enzymes displays some special features. In particular, the rodent ADH2 subgroup of enzymes has low activity, and catalytic efficiency for alcohol oxidation is much lower at physiological pH than at pH 10 (*13*, *15*). To further characterize the enzymatic properties of rodent ADH2 and the mechanistic basis for the low activity, we studied the kinetics of mouse ADH2 and new variants with substitutions at position 47.

Table 4: p*K* Values and pH-Independent Rate Constants for Reactions of Mouse ADH2 Enzymes[a]

enzyme	k_{cat}	k_{cat}/K_m
wild type	$k_1 = 0.36 \pm 0.04$ s^{-1}	$k_1 = 0.82 \pm 0.02$ mM^{-1} s^{-1}
	p$K_a = 8.1 \pm 0.2$	p$K_a = 8.61 \pm 0.05$
Pro47Ala[b]	$k_1 = 5.4 \pm 0.3$ s^{-1}	$k_1 = 18.7 \pm 0.1$ mM^{-1} s^{-1}
	p$K_a = 8.5 \pm 0.1$	p$K_a = 8.47 \pm 0.01$
Pro47Gln	$k_1 = 7.3 \pm 0.2$ s^{-1}	$k_1 = 20.4 \pm 0.7$ mM^{-1} s^{-1}
	p$K_a = 8.24 \pm 0.05$	p$K_a = 8.54 \pm 0.07$
Pro47His	$k_1 = 7.1 \pm 0.3$ s^{-1}	$k_1 = 14.4 \pm 0.5$ mM^{-1} s^{-1}
	p$K_a = 8.39 \pm 0.09$	p$K_a = 9.29 \pm 0.04$

[a] Kinetic constants were determined from initial velocity experiments at 25 °C with varied benzyl alcohol concentrations and the NAD^+ concentration fixed at 2.4 mM. The p*K* values and limiting constants are from fits to eq 1 given in Experimental Procedures. [b] For this enzyme, the data for k_{cat} were fitted somewhat better with eq 2, with the following values: $k_1 = 5.81 \pm 0.07$ s^{-1}, $k_2 = 1.5 \pm 0.2$ s^{-1}, p$K_b = 7.3 \pm 0.1$, and p$K_a = 8.92 \pm 0.05$.

The data from initial velocity and dead-end inhibition studies (Tables 1 and 2) show that the mechanism of mouse ADH2 is consistent with an ordered bi-bi mechanism at pH 7.5. An ordered reaction was also indicated previously for the forward direction at pH 10 (*15*), and human ADH2 follows an ordered bi-bi mechanism (*25*). As shown in Table 3, the isotope effects for oxidation by mouse ADH2 of the protio form as compared to the deuterio form of benzyl alcohol are in the range expected for a mechanism in which hydride transfer is rate-limiting. This has also previously been shown at pH 10 for deuterated octanol (*15*), indicating that hydride transfer is a major rate-determining step for oxidation of different alcohols over a large pH range. With a turnover number of 0.016 s^{-1} for benzyl alcohol and even lower numbers with other substrates, hydride transfer is remarkably slow for mouse ADH2. For comparison, hydride transfer for benzyl alcohol oxidation by horse liver ADH has a rate constant of 24 s^{-1}, i.e., ~3 orders of magnitude larger than that for the mouse enzyme (*26*).

The low activity of the mouse enzyme can be increased by substituting Pro47 with His (*15*). A Pro at this position, which most often is Arg or His and sometimes Gly in other ADHs, is unique for the rodent ADH2 enzymes within the vertebrate ADH family. We generated two additional substitutions at position 47 of the mouse enzyme: Gln, which resembles His in size, hydrophobicity, and ability to form H-bonds, and Ala, which is smaller and neutral. All three mutated ADH2 enzymes had similar turnover numbers for benzyl alcohol oxidation (Table 1), corresponding to an increase of 2 orders of magnitude compared to that of the wild-type enzyme. In addition, the substitutions at position 47 decreased coenzyme affinity 8−51-fold, which might indicate that the rate constants for dissociation of the coenzyme are faster. Nevertheless, the increased activity of the mutated enzymes is ascribed to improved hydride transfer rather than to an increased rate of coenzyme release. For the wild-type enzyme, the rate constant for dissociation of NADH is 37 s^{-1}, which is more than 10-fold higher than the turnover numbers for the mutated mouse enzymes.

Residue 47 has been shown to be important for catalysis and coenzyme binding in studies of variants of human and monkey ADH1 and yeast ADH (*17*−*20*, *27*). Human ADH1B2 (previously named $\beta_2\beta_2$) has His at position 47, and turnover numbers as well as K_m values and dissociation

constants for coenzyme are larger than those of ADH1B1 ($\beta_1\beta_1$) with Arg at this position (*18*). Even faster turnover and lower coenzyme affinity exist with Gln at this position of ADH1B (*18*). For ADH1B, the increase in activity can be ascribed to the faster rate of dissociation of NADH since coenzyme release is rate-limiting. Conversely, wild-type yeast ADH, which has His at the position corresponding to position 47 in ADH1, exhibited slower turnover and higher coenzyme affinity when His was substituted with Arg (*17*). Mouse ADH2 appears to be different from these enzymes because hydride transfer is slower and rate-limiting even for the wild-type enzyme, which binds NADH tightly.

The low activity of wild-type mouse ADH2 could result from a lack of amino acid residues that facilitate deprotonation of the alcohol, which apparently precedes hydride transfer. In horse liver ADH, the p*K* values of zinc-bound alcohols are generally depressed by approximately 9 units as compared to the p*K* values in solution, and thus, the alcohols could form the reactive alkoxides at neutral pH (*28*−*30*). The shift in p*K* values is probably due to the ligation of the alcohol to the catalytic zinc and to the proton relay system, where His51 can act as a general base catalyst in the transfer of a proton from the buried substrate to the bulk solvent (*31*). This seems also to be the case for human ADH1B (*32*). In mouse ADH2, Pro47 and Asn51 are in positions that might participate in proton transfer. However, the previously generated Asn51His substitution in ADH2 did not increase activity, suggesting that an active proton relay system cannot be simply engineered (*15*). Similarly, no increase in activity was obtained with a His51 substitution in the human ADH2 (*33*). For ADHs lacking His at this position, structures of mouse ADH2 (*21*), cod ADH (*34*), and human ADH3 (*35*) suggest an alternative proton relay route involving His47. However, mouse ADH2 does not benefit from introduction of a catalytic base at position 47 since several substitutions at position 47 activate the enzyme to a similar degree, and also exhibit similar pH dependencies (Figure 4). Because the Pro47His substitution did not decrease the p*K* for k_{cat}, and instead increased the p*K* for k_{cat}/K_m by almost 1 unit, as compared to that of the wild type or the other position 47 substitutions (Figure 4 and Table 4), it appears that His47 does not facilitate deprotonation of the zinc ligand. Thus, the higher activity of the mutated mouse enzymes does not appear to be due to improved base catalysis.

All of the mutated ADH2 enzymes display strong pH dependence for alcohol oxidation with the maximal activity at high pH. The p*K* values for k_{cat}/K_m and k_{cat} can be assigned to the ionization of the zinc-bound water and zinc-bound alcohol in the enzyme−NAD^+ and enzyme−NAD^+−alcohol complexes, respectively. The p*K* values for the mouse enzymes are ~2 units higher than those found for the wild-type horse enzyme, but they are similar to the values found for a mutated horse ADH (*36*). The enzyme with the Gly293Ala and Pro295Thr substitutions in the loop containing residues 293−298, which rearranges during the conformational change from the apo- to holoenzyme, maintains the open conformation, leading to increased coenzyme dissociation constants and rate-limiting hydride transfer (*36*). The loop substitutions shift the p*K* values for alcohol oxidation up by 2 units, which apparently results from an impaired ability of His51 to function as a base through the proton relay system. Mouse ADH2 resembles the mutated horse liver ADH in several respects. First, hydride transfer is rate-limiting, although the rate constants are significantly lower for mouse ADH2. Second, mouse ADH2 exhibits similarly high p*K* values (8.6 and 8.1) for both k_{cat}/K_m and k_{cat}, p*K* values that probably correspond to the ionization of the zinc-bound ligand. Third, the ternary complex of mouse ADH2 with NADH and the inhibitor *N*-cyclohexylformamide (an aldehyde analogue) crystallizes in the "semi-open" conformation, i.e., halfway between the open apo and the closed holo complexes of horse ADH1 (*21*). Thus, by analogy to the open conformation observed for the mutated horse liver ADH (*36*), a histidine introduced at position 47 or 51 in mouse ADH2 may not be oriented optimally to act as a catalytic base. Increased accessibility to water or poorly positioned groups in the proton relay system could decrease the effectiveness of a histidine. The structure determined for the Pro47His enzyme is also in a semi-open conformation, and all three mutated enzymes exhibit similar pH dependencies. It appears that in the more open conformations of the enzyme, the zinc ligands ionize without facilitation by a histidine.

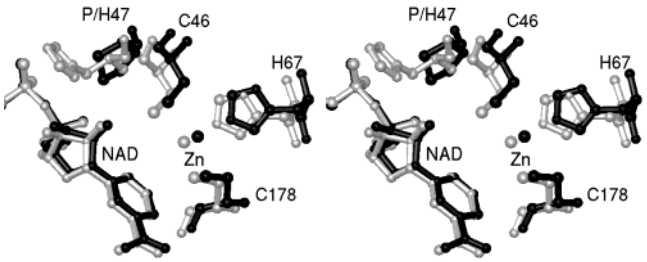

FIGURE 5: Stereodiagram of a comparison of the active sites of wild-type mouse ADH2 (PDB entry 1E3E, dark gray) and the Pro47His mutated enzyme (PDB entry 1E3L, light gray). The coenzyme-binding domains and NADH moieties of each structure were superimposed using O (*37*). The Pro47His structure is more closed than the wild type. This figure was created with Ribbons.

Differences in the mouse ADH2 sequence compared to the corresponding residues in the flexible loop region of the horse enzyme, particularly a two-residue deletion specific for rodent ADH2, may contribute to the structural basis for the more open conformation (*14*, *15*, *21*). Because the active site cleft of mouse ADH2 is more voluminous than in the horse enzyme, the coenzyme and substrate may not be optimally positioned for hydride transfer, and turnover is slower. The increased catalytic efficiency seen when the relatively rigid ring of Pro47 is substituted with another residue appears to result from the active site cleft being more closed, as observed for the Pro47His enzyme (Figure 5). This may produce better positioning of the coenzyme relative to the substrate and the active site residues. Structures of the ternary complex of the Pro47His enzyme have not been determined, but it may be noted that the zinc to which the substrate would bind is closer to the nicotinamide ring of the bound NADH. Although the differences in distance are small, they could affect the rate of hydride transfer.

In conclusion, study of the ADH2 forms of mammalian ADH gives new insights into ADH catalysis. Generally, differences among ADHs affect substrate specificity and coenzyme affinity, which are important for catalytic efficiency. However, within the ADH2 group of enzymes, discrete changes in the topography of the active site

significantly affect the chemical step. Hydride transfer rates are at least 3 orders of magnitude slower for the mouse ADH2 than for horse liver ADH. The low activity of the rodent enzymes probably reflects the semi-open conformation of the enzyme and the increased exposure of the active site to solvent. The positioning of the coenzyme and substrate is not optimal for hydride transfer, but this can be overcome by replacing Pro47, which leads to a more closed conformation and better positioning. Furthermore, hydride transfer requires prior deprotonation of the zinc-bound substrate, which is less efficient for ADH2 (with Pro47 and Asn51) than for other ADHs, but is not affected by substitutions with histidine. Although these studies mostly used benzyl alcohol, since it is a good substrate (*15*), other substrates might have faster hydride transfer rates and lower p*K* values. ADH2 is highly variable, but the mouse and rat forms are 93% identical at the protein level and display almost identical active sites as deduced from the crystal structure of mouse ADH2 (*21*). At this time, the significance of these characteristics for the physiological role(s) of ADH2 is unknown.

REFERENCES

1. Edenberg, H. J., and Bosron, W. F. (1997) in *Comprehensive Toxicology* (Guengerich, F. P., Ed.) pp 119−131, Pergamon Press, New York.
2. Höög, J.-O., Hedberg, J. J., Strömberg, P., and Svensson, S. (2001) *J. Biomed. Sci. 8*, 71−76.
3. Duester, G., Farrés, J., Felder, M. R., Holmes, R. S., Höög, J.-O., Parés, X., Plapp, B. V., Yin, S. J., and Jörnvall, H. (1999) *Biochem. Pharmacol. 58*, 389−395.
4. Theorell, H., and Chance, B. (1951) *Acta Chem. Scand. 5*, 1127−1144.
5. Wratten, C. C., and Cleland, W. W. (1963) *Biochemistry 2*, 935−941.
6. Brändén, C.-I., Jörnvall, H., Eklund, H., and Furugren, B. (1975) in *The Enzymes* (Boyer, P. D., Ed.) pp 103−190, Academic Press, New York.
7. Bosron, W. F., Li, T.-K., Lange, L. G., Dafeldecker, W. P., and Vallee, B. L. (1977) *Biochem. Biophys. Res. Commun. 74*, 85−91.
8. Li, T.-K., Bosron, W. F., Dafeldecker, W. P., Lange, L. G., and Vallee, B. L. (1977) *Proc. Natl. Acad. Sci. U.S.A. 74*, 4378−4381.
9. Estonius, M., Svensson, S., and Höög, J.-O. (1996) *FEBS Lett. 397*, 338−342.
10. Mårdh, G., Dingley, A. L., Auld, D. S., and Vallee, B. L. (1986) *Proc. Natl. Acad. Sci. U.S.A. 83*, 8908−8912.
11. Consalvi, V., Mårdh, G., and Vallee, B. L. (1986) *Biochem. Biophys. Res. Commun. 139*, 1009−1016.
12. Sellin, S., Holmquist, B., Mannervik, B., and Vallee, B. L. (1991) *Biochemistry 30*, 2514−2518.
13. Ditlow, C. C., Holmquist, B., Morelock, M. M., and Vallee, B. L. (1984) *Biochemistry 23*, 6363−6368.
14. Höög, J.-O. (1995) *FEBS Lett. 368*, 445−448.
15. Svensson, S., Strömberg, P., and Höög, J.-O. (1999) *J. Biol. Chem. 274*, 29712−29719.
16. Eklund, H., Nordström, B., Zeppezauer, E., Söderlund, G., Ohlsson, I., Boiwe, T., Söderberg, B. O., Tapia, O., Brändén, C.-I., and Åkeson, Å. (1976) *J. Mol. Biol. 102*, 27−59.
17. Gould, R. M., and Plapp, B. V. (1990) *Biochemistry 29*, 5463−5468.
18. Hurley, T. D., Edenberg, H. J., and Bosron, W. F. (1990) *J. Biol. Chem. 265*, 16366−16372.
19. Stone, C. L., Bosron, W. F., and Dunn, M. F. (1993) *J. Biol. Chem. 268*, 892−899.
20. Light, D. R., Dennis, M. S., Forsythe, I. J., Liu, C.-C., Green, D. W., Kratzer, D. A., and Plapp, B. V. (1992) *J. Biol. Chem. 267*, 12592−12599.
21. Svensson, S., Höög, J.-O., Schneider, G., and Sandalova, T. (2000) *J. Mol. Biol. 302*, 441−453.
22. Deng, W. P., and Nickoloff, J. A. (1992) *Anal. Biochem. 200*, 81−88.
23. Cleland, W. W. (1979) *Methods Enzymol. 63*, 103−138.
24. Frieden, C. (1994) *Methods Enzymol. 240*, 311−322.
25. Bosron, W. F., Li, T. K., Dafeldecker, W. P., and Vallee, B. L. (1979) *Biochemistry 18*, 1101−1105.
26. Sekhar, V. C., and Plapp, B. V. (1990) *Biochemistry 29*, 4289−4295.
27. Jörnvall, H., Hempel, J., Vallee, B. L., Bosron, W. F., and Li, T.-K. (1984) *Proc. Natl. Acad. Sci. U.S.A. 81*, 3024−3028.
28. Kvassman, J., and Pettersson, G. (1978) *Eur. J. Biochem. 87*, 417−427.
29. Kvassman, J., and Pettersson, G. (1980) *Eur. J. Biochem. 103*, 557−564.
30. Kvassman, J., Larsson, A., and Pettersson, G. (1981) *Eur. J. Biochem. 114*, 555−563.
31. Eklund, H., Plapp, B. V., Samama, J.-P., and Brändén, C.-I. (1982) *J. Biol. Chem. 257*, 14349−14358.
32. Ehrig, T., Hurley, T. D., Edenberg, H. J., and Bosron, W. F. (1991) *Biochemistry 30*, 1062−1068.
33. Davis, G. J., Carr, L. G., Hurley, T. D., Li, T.-K., and Bosron, W. F. (1994) *Arch. Biochem. Biophys. 311*, 307−312.
34. Ramaswamy, S., el Ahmad, M., Danielsson, O., Jörnvall, H., and Eklund, H. (1996) *Protein Sci. 5*, 663−671.
35. Yang, Z. N., Bosron, W. F., and Hurley, T. D. (1997) *J. Mol. Biol. 265*, 330−343.
36. Ramaswamy, S., Park, D.-H., and Plapp, B. V. (1999) *Biochemistry 38*, 13951−13959.
37. Jones, T. A., Zou, J., Cowan, S., and Kjeldgaard, M. (1991) *Acta Crystallogr. A47*, 110−119.

BI0354482